JOURNAL OF VIROLOGY, Aug. 2009, p. 7842–7849 Vol. 83, No. 16
0022-538X/09/$08.00+0 doi:10.1128/JVI.00309-09

The Nucleoprotein of Lymphocytic Choriomeningitis Virus Facilitates Spread of Persistent Infection through Stabilization of the Keratin Network▽

Martina Labudova,[1] Jana Tomaskova,[1] Ludovit Skultety,[1,2] Jaromir Pastorek,[1] and Silvia Pastorekova[1,2]*

Institute of Virology, Slovak Academy of Sciences, Dubravska cesta 9, 845 05 Bratislava,[1] and Centre for Molecular Medicine, Vlarska 3-7, 831 01 Bratislava,[2] Slovak Republic

Received 12 February 2009/Accepted 22 May 2009

Lymphocytic choriomeningitis virus (LCMV) is a prototypic arenavirus containing a bisegmented single-stranded RNA genome with an ambisense coding strategy. MX is a noncytolytic LCMV strain with an in vitro host range restricted to only few cell lines. MX LCMV spreads via cell-cell contacts and causes persistent infection with high production of viral nucleoprotein (NP). Using a proteomic approach, we identified keratin 1 (K1), an intermediate filament network component, as a binding partner of the viral NP. The functional significance of this interaction has been examined by chemical disruption of the keratin network, resulting in a reduced spread of MX LCMV in HeLa cells. However, K1 disassembly was considerably lower in MX LCMV-infected cells than in noninfected counterparts, indicating that NP can stabilize the keratin network and thereby support the integrity of cytoskeleton. The presence of NP also resulted in increased formation of desmosomes and stronger cell-cell adhesion. Similar effects were observed in HeLa cells persistently infected with LCMV strain Armstrong. Our findings suggest that the keratin network is important for the intercellular transmission of persistent LCMV infection in epithelial cells and show that the virus can actively facilitate its own intercellular spread through the interaction between the viral NP and K1 and stimulation of cell-cell contacts.

Lymphocytic choriomeningitis virus (LCMV) is a prototypic arenavirus with bisegmented single-stranded RNA genome. Both segments (small [S] and large [L]) contain two open reading frames in mutually opposite orientations and utilize an ambisense coding strategy (19). The S RNA encodes a major viral protein nucleoprotein (NP) and a glycoprotein precursor (GP-C), which is cotranslationally cleaved into peripheral glycoprotein 1 (GP1) and transmembrane glycoprotein 2 (GP2) (30). The L RNA segment encodes an RNA-dependent RNA polymerase (L) and a regulatory ring finger Z protein (ZP) (2, 26). Virus replication starts with the L polymerase-driven transcription of the 3′ RNA genome arms of negative polarity and produces mRNAs that are subsequently translated to NP and L polymerase. These viral proteins assist in the transcription of the RNA genome to virus cRNA, serving as a template for the synthesis of the new genomic RNA molecules as well as for the subgenomic mRNAs translated to GP-C and ZP (2, 19). This unusual two-stage replication strategy facilitates establishment of virus persistence, which can be sustained by the virus ribonucleoprotein composed of NP, the RNA genome, and L polymerase in the absence of mature virion production caused by absent or limited expression of glycoproteins (2, 33). LCMV can easily set up persistent infection in a wide variety of cell types derived from various species, where it does not perturb vital cell functions but modulates nonessential phenotypic features (20, 22, 33).

In vivo, LCMV readily causes persistent infection of common house mouse (*Mus musculus*), its natural host and reservoir. Humans are generally infected through the respiratory tract after direct or indirect contact with infected rodents or pets. In immunocompetent individuals, LCMV causes illnesses varying from mild flu-like symptoms to rare severe encephalitis (15, 22). Infection with this virus during pregnancy has been linked to spontaneous abortions and malformations (16). More strikingly, fatal cases of LCMV infections transmitted via transplanted organs from infected donors to immunosuppressed recipients were recently reported and call for more attention to this seemingly innocent virus (1, 7).

The MX strain of LCMV was originally identified in the human MaTu cell line, which was presumably derived from a mammary tumor as described earlier (21, 25). Analysis of the MX LCMV coding regions has revealed sequence differences supporting the view that MX is a separate LCMV strain (9, 25, 32). MX LCMV does not cause any cellular damage, and its host range is restricted to only few cell lines. It is transmissible by direct cell-to-cell contact or cell extract but not by filtered medium of infected cells (25). Furthermore, cells infected with MX LCMV accumulate high cytoplasmic levels of NP and ZP and contain deleted RNAs (9, 25, 32).

Despite NP being the most abundant viral protein expressed in persistently infected cells and a major component of the minimal infection unit of the virus with a central role in transcription and replication of the LCMV genome (23), there are no data available on its functional involvement in noncytolytic

* Corresponding author. Mailing address: Institute of Virology, Slovak Academy of Sciences, Dubravska cesta 9, 845 05 Bratislava, Slovak Republic. Phone: 421-2-59302404. Fax: 421-2-54774284. E-mail: virusipa@savba.sk.

▽ Published ahead of print on 3 June 2009.

LCMV spread. Since persistent infection relies on cooperation of the virus components with the molecular machinery of an infected cell, we decided to employ a proteomic approach to identify the molecular partner(s) of NP using MX LCMV persisting in human HeLa cells as a model. Here we demonstrate that MX NP binds and stabilizes keratin 1 (K1), a part of an intermediate filament network, and thereby facilitates LCMV transmission via cell-to-cell contacts. Although different viruses are known to depend on cytoskeleton components that assist their transmission to noninfected cells (24, 28), this is the first example of an active modulation of the keratin network stability involved in the spread of persistent infection.

MATERIALS AND METHODS

Viruses and cells. LCMV strain MX was continuously propagated in persistently infected HeLa cervical carcinoma cells designated HeLa-MX (25). The infection was established using a cell extract from MaTu cells prepared by the procedure of van der Zeijst et al. (25, 33). Persistent infection with LCMV strain Armstrong (kindly provided by Boris Klempa, Institute of Virology, Slovak Academy of Sciences, Bratislava) was started by virus adsorption at a multiplicity of 0.1 PFU. During the initial acute phase, dead cells were removed and fresh HeLa cells were added until signs of cytopathic effect disappeared. The persistently infected HeLa-ARM cells were regularly split, and spread of the virus was verified by immunofluorescence using an anti-NP monoclonal antibody (MAb) as described below. Noninfected HeLa cells cultured in parallel were used as a control. The cells were grown in Dulbecco's modified Eagle medium supplemented with 10% fetal bovine serum, 2 mM L-glutamine (Lonza, Verviers, Belgium), and 160 μg/ml gentamicin (Lek, Ljubljana, Slovenia) in a humidified air atmosphere at 37°C in the presence of 5% CO_2. The cultures were maintained at high cell density to allow for easier virus transmission via cell-to-cell contacts.

Antibodies. Mouse MAbs M16 and M67, specific for the NP of LCMV, were described earlier (21, 25). Anti-K1 affinity-purified goat polyclonal immunoglobulin G (IgG) antibody N-20, raised against a peptide mapping within an internal region of the human K1, was used at a 1:200 dilution (Santa Cruz, Santa Cruz, CA). Mouse MAb clone ZK-31, specific for desmosomes (but not hemidesmosomes), was used at a 1:300 dilution (Sigma Aldrich, St. Louis, MO). Anti-β-actin MAb (Sigma Aldrich) was used for a loading control. Swine anti-mouse IgG conjugated with horseradish peroxidase and diluted 1:5,000 (SEVAC, Prague, Czech Republic) and donkey anti-goat IgG conjugated with horseradish peroxidase and diluted 1:5,000 (Dako, Glostrup, Denmark) were used for immunoblotting analyses. Horse anti-mouse IgG (heavy plus light chains) conjugated with fluorescein isothiocyanate and diluted 1:300 (Vector Laboratories, Peterborough, England) and rabbit anti-goat IgG conjugated with Alexa Fluor 594 and diluted 1:2,000 (Advanced Targeted Systems, San Diego, CA) were used for confocal microscopic analyses.

Plasmids. NP cDNA was obtained by reverse transcription-PCR amplification of the MX LCMV NP gene using the primers NP sense (5′-CCGAATTCATG TCTCTGTCCAAGGAAGTCA-3′) and NP antisense (5′-CCTCGAGTTAGA GTGTCACAACATTTGGTC-3′). The DNA fragment was cloned via EcoRI and XhoI cleavage sites (underlined) using standard procedures into the pGEX-4T1 prokaryotic expression vector (GE Healthcare, Little Chalfont, United Kingdom). The resulting construct was verified by sequencing.

Pull-down assay. Expression of glutathione *S*-transferase (GST)–NP fusion protein and its affinity purification on glutathione-S Sepharose beads were done as described previously (4). HeLa cells were either metabolically labeled overnight at 37°C with [^{35}S]methionine-cysteine using Promix ^{35}S (GE Healthcare) or used without labeling. The cells were lysed in radioimmunoprecipitation assay buffer with inhibitors of proteases (Complete Mini protease inhibitor cocktail tablets; Roche Applied Science, Basel, Switzerland) and phosphatases (1 and 2; Sigma), incubated on ice for 15 min, and centrifuged for 15 min at 15,000 rpm. The pull-down assay was done with 5 μg of GST-NP bound to glutathione-S Sepharose and incubated with HeLa extracts for 1 h at 4°C. After extensive washing with saline Tris-EDTA buffer, samples containing bound proteins were separated by 10% sodium dodecyl sulfate-polyacrylamide gel electrophoresis (SDS-PAGE). Gels were either stained with a silver staining kit (GE Healthcare) or dried and exposed to Fuji film.

Protein identification by tandem mass spectrometry. Selected protein bands were excised from the gel and destained. Gel plugs were dehydrated in 100% acetonitrile for 5 min, and the proteins in the gel were reduced (10 mM dithiothreitol), alkylated (55 mM iodoacetamide), and digested with 0.1 μg trypsin (Promega, Madison, WI) in 50 mM ammonium bicarbonate buffer (pH 7.8) overnight at 37°C. The resulting peptides were extracted twice with 50 μl of extraction solution (60% acetonitrile, 1% formic acid) during agitation for 10 min. Pooled extracts were transferred to microplates and dried by lyophilization. The extracted peptide mixture was dissolved in 20 μl of 2% acetonitrile in water with addition of 0.1% of formic acid and separated with a nanoAcquity UPLC system (Waters, Milford, MA) as described previously (14). The data acquisition was performed in data-dependent manner for the time of the separation, collecting up to three tandem mass spectrometry events at the same time. Data were processed by ProteinLynx Global Server v. 2.2 (Waters), which provided background subtraction (polynomial order, 5; threshold, 35%), smoothing (Savitzky Golay, twice, over three channels), and centroiding (top, 80%; minimal peak width at half height, 4). The resulting data were searched against the human NBCI database under the following criteria: fixed carbamidomethylation of Cys, variable Met oxidation, tryptic fragments with one miss cleavage, peptide mass tolerance of 50 ppm, and fragment mass tolerance of 0.05 Da. The results were validated by the identification of three or more consecutive fragment ions from the same series. The protein assignments with at least two peptides matching the theoretical sequences were considered positively identified.

Coimmunoprecipitation and Western blotting. Protein A-Sepharose (GE Healthcare) was washed three times with phosphate-buffered saline (PBS). Radioimmunoprecipitation assay lysates obtained from confluent HeLa-MX and HeLa cells were precleared with a 50% protein A-Sepharose slurry. Antibody was bound at room temperature for 2 h. Immunocomplexes were allowed to form at 4°C overnight. Beads were washed five times in PBS and centrifuged. Samples were resolved by 10% SDS-PAGE. The proteins were transferred onto a polyvinylidene difluoride membrane (Immobilon-P; Millipore, Billerica, MA). The Western blot was incubated with N-20 anti-K1 or M67 anti-NP antibodies as described previously (13, 21). Proteins were detected by using the ECL detection system.

Immunofluorescence and confocal microscopy. Cells grown on glass coverslips were washed with PBS, fixed with methanol for 5 min at −20°C, washed again, and saturated with 3% bovine serum albumin for 30 min at 37°C (Applichem, Kongens Lyngby, Denmark). The cells were incubated with primary antibody for 1 h at 37°C, washed four times with PBS containing 0,2% Tween 20, and treated for 1 h at 37°C with the secondary antibody diluted in 1% bovine serum albumin. The cells were washed again with PBS containing 0.2% Tween 20. Nuclei were stained with DAPI (4′,6′-diamidino-2-phenylindole) (Sigma-Aldrich). Coverslips were mounted with fluorescein FragEL mounting medium (Calbiochem, Darmstadt, Germany), viewed on Zeiss LSM 510 confocal microscope, deconvoluted with Huygens essential software, and analyzed with ImageJ software.

Aggregation assay. Cells seeded into a 24-well plate (1.5×10^5 cells/well) were grown for 3 days to form dense monolayers. The monolayers were then washed and trypsinized. Single-cell suspensions were transferred into a 24-well plate with a nonadhesive surface and rotated for 20 h at 37°C on a gyratory shaker at 100 rpm to allow for spontaneous aggregation. Cell aggregates were viewed with a Precision inverted microscope (World Precision Instruments, Berlin, Germany) and photographed using an Olympus OM-4TI camera.

Inhibition of virus transmission by disruption of the keratin network. A mixture of 300,000 infected and uninfected cells at a 1:10 ratio was seeded on a 24-well plate and allowed to adhere for 24 h. On the next day, 2 mM EGTA was added, left for 15 min, and replaced by fresh medium, and cells were allowed to recover for 24 h; the treatment was repeated twice. After each treatment-recovery cycle, cells in three parallel wells were fixed with methanol for 5 min at −20°C and analyzed by immunofluorescence using either anti-NP antibody combined with anti-K1 antibody or antidesmosome antibody combined with anti-K1 antibody. For assessment of viability, the nonfixed cells were labeled with ViaCount solution according to instructions of the manufacturer (Guava Technologies, Hayward, CA), measured on a Guava flow cytometer, and analyzed by the ViaCount program. Alternatively, the nonfixed cells were stained with 50 μM propidium iodide (Sigma Aldrich) in PBS for 5 min at room temperature, and dead cells that accumulated the dye were examined under a Precision inverted microscope.

RESULTS

MX LCMV NP interacts with K1. To identify potential binding partners, MX LCMV NP was expressed as a GST-NP fusion protein, immobilized on glutathione-S Sepharose beads, and allowed to interact with the proteins extracted from unin-

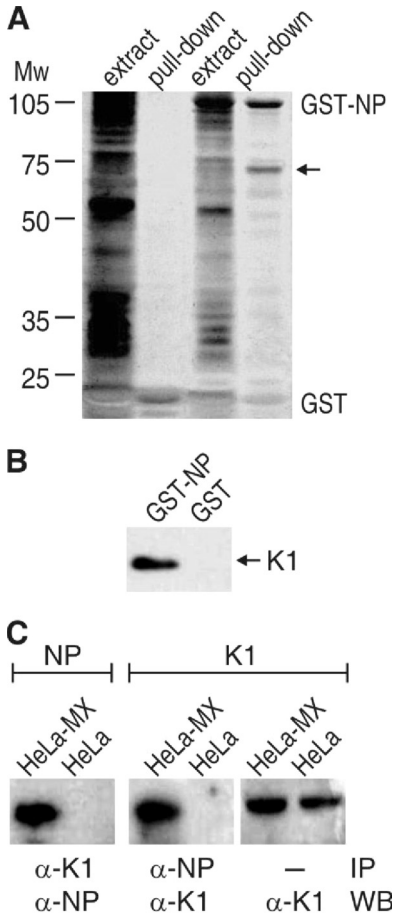

FIG. 1. Identification of K1 as an interacting partner of MX LCMV NP. (A) Pull-down assay. GST-NP fusion protein and GST were immobilized on glutathione-S Sepharose and incubated with extracts from HeLa cells. Proteins bound to GST-NP and GST were separated by SDS-PAGE, and whole extracts were loaded for the control of input. A prominent band corresponding to 70 kDa was detected among GST-NP pulled-down proteins (arrow) and identified by sequencing as K1. (B) Pull-down assay combined with Western blotting and immunodetection of K1. (C) Immunoprecipitation combined with Western blotting was performed as a proof of interaction between virus NP and K1. The antibodies used for each step are indicated at the bottom.

fected HeLa cells. GST alone was produced in parallel and used as a negative control. The proteins bound to GST-NP versus GST alone were then resolved by SDS-PAGE (Fig. 1A). Electrophoretic analysis revealed that GST-NP selectively bound a protein with the molecular mass of about 70 kDa. The tryptic digest of the protein band was analyzed by electrospray tandem mass spectrometry. The amino acid sequence of the SLDLDSIIAEVK peptide fully corresponded to the type II K1 (P04264; K2C1_HUMAN), a component of the intermediate filament network, suggesting that NP interacts with K1.

To confirm this interaction, the pull-down assay with GST-NP and GST control was repeated using extracts from ^{35}S-labeled cells (data not shown) and also analyzed by Western blotting using anti-K1 antibody. In accordance with the initial experiment, a K1-specific band was detected only in the sample containing GST-NP and not in the sample with GST alone (Fig. 1B). We also performed coimmunoprecipitation experiments using protein extracts from MX-infected HeLa cells with anti-K1 antibody employed in the precipitation step and anti-NP antibody in the detection of interacting NP on the Western blot and vice versa. As shown in Fig. 1C, NP was coimmunoprecipitated with anti-K1 antibody and K1 was coimmunoprecipitated with anti-NP antibody from HeLa-MX extract, further proving the interaction between these two proteins. Finally, the interaction between NP and K1 was verified by far-Western blotting (data not shown).

NP colocalizes with K1 and supports formation of desmosomes. In the next step, we decided to investigate whether interaction between NP and K1 could be observed at the level of colocalization. In addition, we wanted to analyze the overall organization of the keratin network in LCMV-infected versus noninfected HeLa cells. For this purpose, we used double-staining immunofluorescence analysis by confocal microscopy in which the K1 network was visualized with the goat anti-K1 antibody followed by anti-goat IgG labeled with Alexa Fluor 594 (red) and NP was detected with the mouse anti-NP MAb followed by FITC-labeled anti-mouse IgG (green). The staining patterns for K1 and NP in infected cells were similar, and their signals revealed a significant overlap, suggesting that NP is associated with the K1 network (Fig. 2 A and B).

Interestingly, the K1 distribution in MX LCMV-infected HeLa cells differed from its distribution in the control noninfected cells (Fig. 2 A). In HeLa cells, K1 was located predominantly in the cytoplasm close to the nucleus but was generally absent in periplasmic areas. On the other hand, in HeLa-MX cells, K1 was more evenly distributed all over the cells. It was also clearly seen in cellular protrusions. Moreover, both Western blotting analysis and immunofluorescence staining have shown that the K1 content was higher in the infected cells than in the noninfected counterparts (Fig. 1C and 2A), and the keratin network was more prominent even in nonstained HeLa-MX cells (Fig. 2C).

In epithelial cells, K1 is anchored to desmosomes, which are important components of the intercellular junctional contacts (12). Both the keratin filaments and desmosomes act in concert as mechanosensory devices involved in regulation of cell adhesion-related processes (12). We therefore investigated whether MX LCMV NP interaction with K1 affects the formation of desmosomes in HeLa cells, which originate from carcinoma and thus have reduced capacity to form cell-cell adhesions (3). Indeed, noninfected HeLa cells revealed very rare desmosome-specific staining signal mostly confined to perinuclear cytoplasmic areas (Fig. 3A). In contrast, MX LCMV-infected HeLa cells showed a strong punctuated signal that was clearly localized at the interfaces of neighboring cells as typical for desmosomes (Fig. 3A). This finding suggested that the infected cells were able to organize their keratin network into scaffolds involved in desmosome-mediated cell-cell adhesion. In support of this conclusion, infected HeLa-MX cells showed a considerably higher cell-cell adhesion capacity as analyzed by cell aggregation assay (Fig. 3B).

In addition, we evaluated the extent of K1 assembly in infected HeLa-MX cells compared to noninfected HeLa controls. The soluble fraction and insoluble pellet of the cell lysates were separately analyzed by Western blotting. In accordance with the results of adhesion assays, HeLa cells showed a higher level of soluble K1, whereas HeLa-MX cells

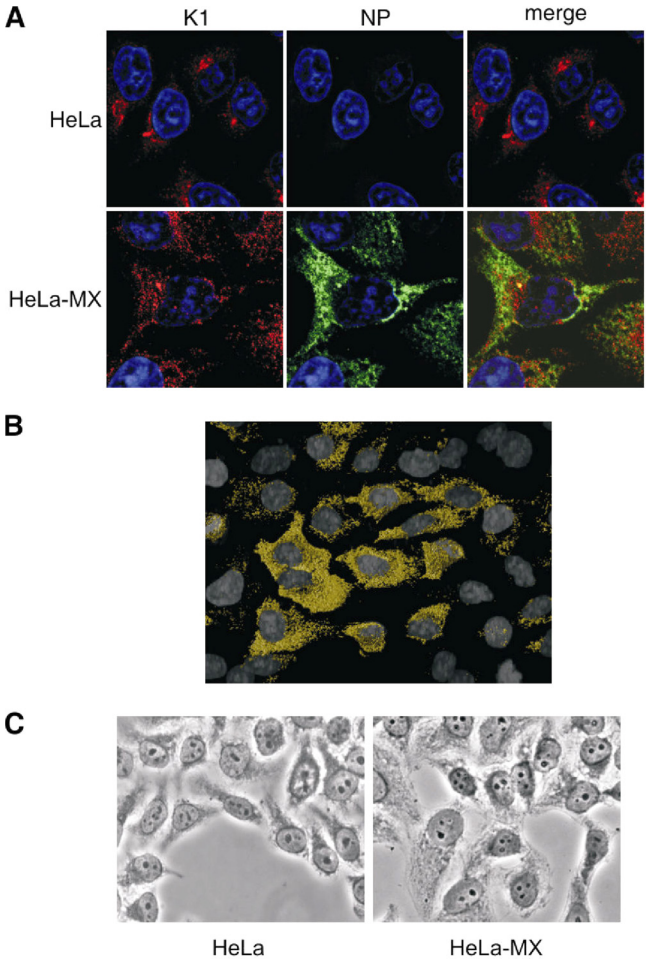

FIG. 2. The K1 network in infected versus noninfected HeLa cells. (A) Immunofluorescence detection of K1 in HeLa-MX cells in comparison with noninfected HeLa controls and colocalization with MX LCMV NP using K1-specific (red) and NP-specific (green) MAbs. Cell nuclei were stained with DAPI (blue). HeLa-MX cells containing NP display a higher content and better organization of K1. Original magnification, ×63. (B) Three-dimensional colocalization map of NP and K1 signals obtained from double-staining confocal analysis of mixed HeLa and HeLa-MX monolayer. The figure shows only the sites where NP and K1 overlap in MX LCMV-infected cells (Pearson's coefficient of colocalization corresponds to 0.704). The colocalization signal is absent from noninfected cells containing only K1 and no NP. (C) Phase-contrast micrographs show a more prominent keratin network in MX LCMV-infected cells.

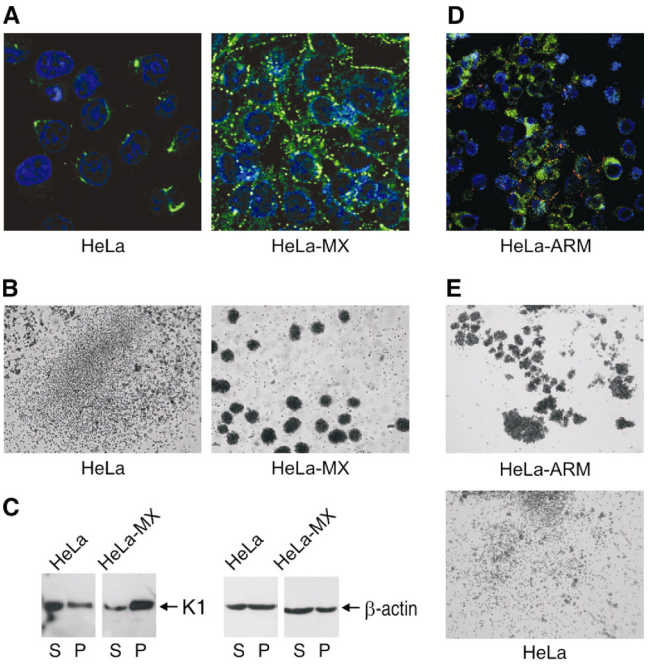

FIG. 3. Formation of desmosomes in MX LCMV-infected HeLa cells. (A) Immunofluorescence analysis of desmosomes using the specific MAb ZK-31 (green) revealed a lack of desmosomal signal in noninfected HeLa cells. In contrast, HeLa-MX cells showed strong staining signals with a pattern typical for desmosomes. Cell nuclei were stained with DAPI (blue). (B) HeLa-MX cells also exhibited increased cell adhesion capacity in an assay based on spontaneous aggregation of cells first grown in a monolayer and then brought to single-cell suspension, placed on a nonadhesive surface, and rotated overnight on a gyratory shaker. (C) K1 assembly in soluble (S) and pellet (P) fractions of the cell extracts was analyzed by Western blotting. β-Actin was detected as a loading control. (D) Double-staining immunofluorescence analysis of viral NP (green) and desmosomes (red) in HeLa cells persistently infected with LCMV strain Armstrong. Infected cells show a clear desmosomal signal which is absent from noninfected counterparts. (E) An aggregation assay of infected HeLa-ARM cells compared to noninfected control HeLa cells confirmed increased clustering of infected cells.

contained more K1 in the insoluble fraction, suggesting a higher degree of its assembly (Fig. 3C).

Interestingly, increased desmosome formation and cell-cell adhesion capacity were also observed in HeLa cells persistently infected with LCMV strain Armstrong, suggesting that this phenomenon is not strain specific but is generally relevant to LCMV (Fig. 3D and E).

MX LCMV infection protects the keratin network and desmosomes against disassembly. Based on the above-described results, it appeared plausible that the interaction between the viral NP and K1 ensures better organization and stabilization of the keratin network. To test this assumption, we utilized chemicals known to cause disassembly of the keratin filaments, including EGTA, acrylamide, and ocadaic acid (27), and observed their effects on distortion of K1 and disruption of desmosomes. EGTA treatment of noninfected HeLa monolayers resulted in almost complete disappearance of the keratin filaments, with traces of immunoreactive K1 around the nucleus (Fig. 4B). On the other hand, MX LCMV-infected cells showed a relatively well preserved keratin network. Although part of K1 bundles was retracted toward the nucleus, the other part remained close to the membrane, consistent with the partially preserved desmosomes (Fig. 4B). Similar effects were observed upon treatments with acrylamide (Fig. 4C) and ocadaic acid (data not shown).

Keratin network distortion blocks the spread of persistent MX-LCMV infection. Several viruses were shown to increase their intercellular spread by maximizing intercellular contacts, usually through manipulating actin polymerization (6, 10). On the other hand, forced disassembly of the actin network was shown to reduce virus transmission. Because keratins cooperate with actin in the formation of fully functional, dynamic cytoskeleton of epithelial cells (11), we investigated whether a

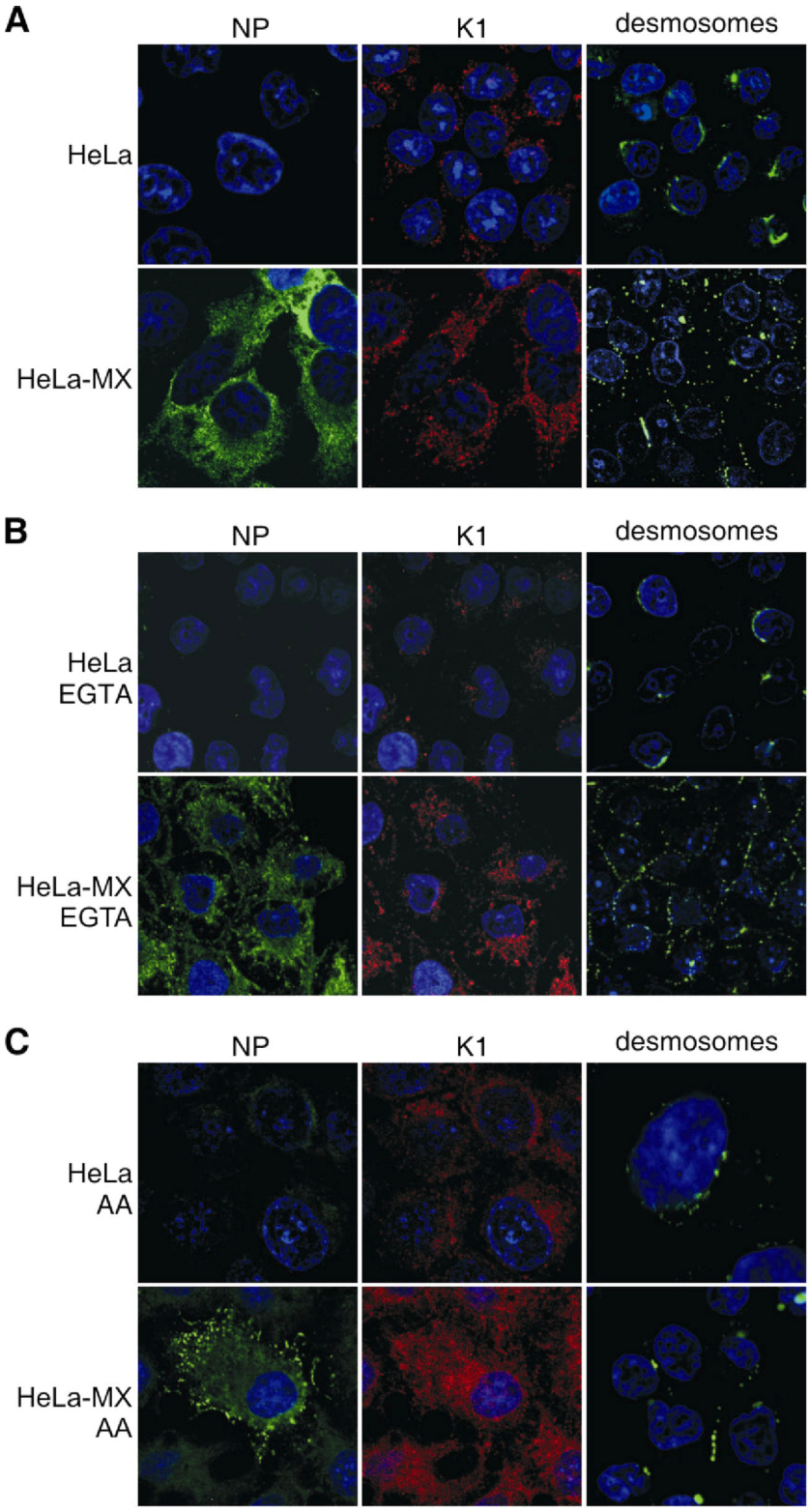

FIG. 4. Effect of keratin network disassembly on distribution of NP, K1, and desmosomes, showing immunofluorescence analysis of control HeLa and HeLa-MX cells (A) and of cells treated with the inhibitors of intermediate filaments EGTA (B) and acrylamide (AA) (C). The cells were treated for 15 min with 2 mM EGTA and for 8 h with 5 mM AA, and then they were fixed and stained with antibodies specific for NP (green), K1 (red), and desmosomes (green). Cell nuclei were stained with DAPI (blue). Both inhibitors caused a loss or reduction of K1 and desmosomal staining signals in the noninfected cells, whereas these signals were relatively well preserved in the infected cells. Original magnification, ×63.

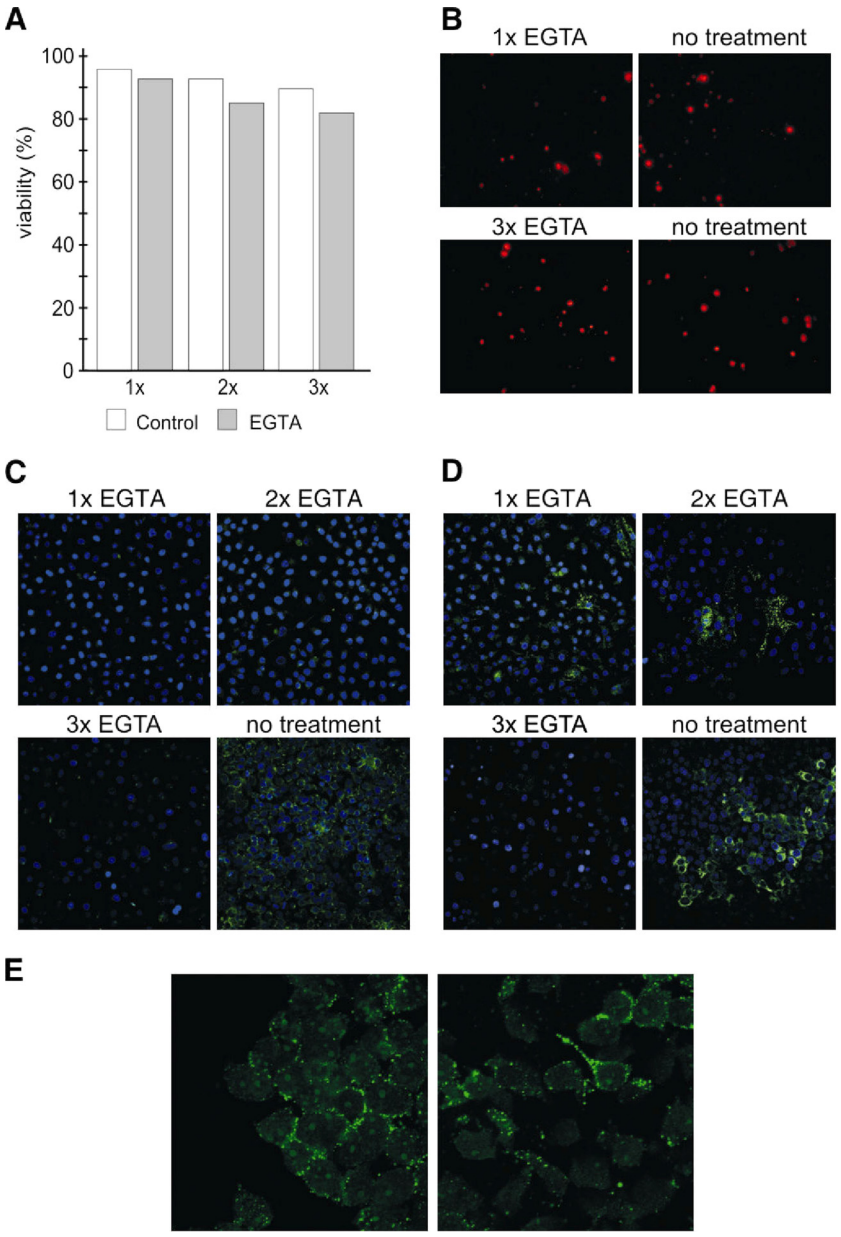

FIG. 5. Effect of keratin network disassembly and loss of cell-cell contacts on MX LCMV spread in HeLa cells. Immunofluorescence analysis of HeLa cells mixed with HeLa-MX cells in a 10:1 ratio was used to detect MX LCMV spread. (A and B) The mixed cell monolayers were treated with EGTA, and the viability of cells was assessed by flow cytometric analysis (A) and by fluorescence microscopy of cells stained with propidium iodide (B) as described in Materials and Methods. (C and D) For analysis of MX LCMV spread, the cells were stained with desmosome (C)- and NP (D)-specific antibodies. EGTA was added to cells and left for 15 min once, twice, or three times, with 24-h recovery periods between the treatments. Untreated cells were maintained in parallel. In the absence of EGTA treatment, clusters of neighboring cells show the presence of desmosomes and NP, suggesting that the virus was spread via cell-cell contacts. In contrast, virtually no desmosomes are visible in EGTA-treated cells, and the NP signal is either confined to few isolated cells or completely absent from the monolayer. Original magnification, ×10. (E) In order to show that LCMV spread is affected by disruption of intercellular contacts (as a consequence of disruption of the keratin network), we stained nonfixed cells with NP-specific antibody. Because antibody cannot cross the membranes of living cells, it could bind only to NP present on the cell surface as a component of minimal infection units. The figure shows that NP can be detected on the cell surface and that the signal is concentrated in the areas of intercellular contacts. On the other hand, it is not visible when cell-cell contacts are missing.

disruption of the cytoskeleton could interfere with the transmission of MX LCMV in HeLa cells. Therefore, we used EGTA as an agent promoting reorganization and disassembly of keratin filaments to treat the infected HeLa-MX cells seeded in a mixed culture with the noninfected HeLa cells. The viability of cells treated with EGTA was monitored by flow cytometric analysis and fluorescence microscopy. As shown in Fig. 5A and B, EGTA did not have any significant effect on cell viability. We then examined the effect of EGTA on the presence of desmosomes, which associate and cooperate with ker-

atin filaments. EGTA-treated HeLa-MX cells did not show any staining with a desmosome-specific antibody and were apparently unable to form desmosomes (Fig. 5C). In contrast, nontreated control cells revealed a punctuated staining pattern typical for desmosomes. We also detected the viral NP, which could be produced only in the infected cells and therefore indicated virus spread. As expected, MX LCMV NP was clearly visible in the nontreated samples in the form of large clusters of cells stained with NP-specific MAb (Fig. 5D). On the other hand, the corresponding samples of cells treated with EGTA once or twice showed only a few NP-positive cells scattered through the culture, and no NP-positive cells were found in the cells treated three times (Fig. 5D). Interestingly, NP was detected on the surface of living cells, presumably as a component of minimal infection units, and was confined to cell-cell contacts (Fig. 5E). This result clearly suggested that MX LCMV spread was inhibited following EGTA-mediated disassembly of intermediate filaments and that the virus depends on the correct organization of the keratin network and formation of cell-cell contacts. It also indicates that the interaction between virus NP and cellular K1 leading to stabilization and better organization of the keratin network plays an important role in the intercellular transmission of persistent LCMV infection.

DISCUSSION

An increasing body of evidence suggests that viruses can efficiently spread along cell membrane protrusions using different types of intercellular connections (17, 28). Such a mode of spread offers several advantages: the viruses can avoid the rate-limiting step of diffusion, decrease the distance to noninfected target cells, reduce the exposure to environmental factors and immune defense mechanisms, and in some cases circumvent the requirement for receptors. In addition, this route of transmission can be utilized also for viruses that remain largely cell associated. For example, human immunodeficiency virus can be transmitted between T cells via cellular contact points known as virological synapses or through recently described membrane nanotubes (8, 31). Murine leukemia virus moves along the outer surface of filopodial bridges (29). Accelerated spread via intercellular contacts is also exploited by poxviruses and herpesviruses (17).

However, viruses not only utilize existing intercellular contacts to move directionally inside and across different tissues but also actively support the formation of membrane protrusion, filopodia, different junctions, and synaptic structures. They employ various strategies, including actions of different viral components that induce budding at the infected cell-target cell interface and/or actin or tubulin polymerization (28). For example, the US3 kinase of pseudorabies virus induces large, tubulin-filled cytoplasmic extensions similar to axons (6); murine herpesvirus 68 gp48 in cooperation with ORF58 stimulates the outgrowth of long, branched plasma membrane fronds to create an intercellular network for virion traffic (10); and vaccinia virus operates via the A36R viral factor, which is involved in actin polymerization and formation of comet tails that propel virions toward the noninfected cell (35). These strategies serve to promote virus spread and are therefore very important for the outcome of the viral infections, especially in cell and tissue types such as nerve or immune cells, which do not communicate via classical mechanisms of cell adhesion but rely on transient mode of intercellular contacts.

In this paper we show yet another strategy for cell-cell virus transmission, which was revealed as a result of the proteomic identification of the type II K1 as a binding partner of the LCMV NP. LCMV readily causes persistent infections characterized by increased production of NP and ZP, reduced production (and/or aberrant processing) of virus glycoproteins, and an absence of mature extracellular virions. Therefore, the spread of persistent, cell-associated LCMV infection in culture depends largely on intercellular connections that mediate continuity between neighboring cells. This has been particularly shown for the MX strain of LCMV, which is noncytolytic and cannot be transferred to noninfected cells by filtered extracellular medium. It is noteworthy that intact MX-infected HeLa cells show NP staining signals at the extracellular side of the plasma membrane, suggesting that they are able to produce defective cell surface-associated particles. In these cells, persistent MX LCMV infection could be maintained by continuous growth in a high-density monolayer in which the cells are closer to each other. However, despite the epithelial origin, HeLa cells do not express several components of cell-cell adhesion machinery and are unable to establish classical epithelial cell-cell contacts, similarly to many other carcinoma cells. This is clearly demonstrated by their inability to form desmosomes, which are specialized cell junctions important for the maintenance of integrity of the normal epithelial tissues. Interestingly, persistent infection of these cells with MX LCMV (and similarly with LCMV strain Armstrong) led to the appearance of a typical desmosomal staining signal at the interface of neighboring infected cells, supporting reestablishment of desmosomal contacts and increased cell aggregation. In accordance with the fact that desmosomes are physically and functionally interconnected with keratin filaments, the infected cells also showed a more even distribution of K1, reaching the submembrane cytoplasmic region at the cell periphery and extending toward cellular protrusions. The presence of MX LCMV NP was also associated with increased formation of these protrusions, which were particularly visible between the spatially separated infected cells. Moreover, the NP itself was present at the intercellular connection, suggesting that it has contributed to formation of these connections, presumably via direct interaction with K1. However, at this stage it is difficult to judge whether NP alone is capable of triggering all of the observed effects or whether it cooperates with other virus components. Further investigation is required to resolve this issue.

Although keratins are generally perceived as relatively rigid protein scaffolds protecting the epithelial cells against mechanical stress, recent advances show that they cross talk with the dynamic actin filaments and microtubules and actively contribute to different aspects of cell behavior, including signal transduction, cell differentiation, proliferation, and migration (18). Keratin filaments show a high degree of flexibility, especially at the cell periphery at sites of focal adhesions, where they can be formed and grow toward the leading edge of the cell (34). Therefore, it is quite conceivable that keratins could also support the formation or stabilization of actin- or microtubule-

containing cellular protrusions generated in order to promote the intercellular spread of persistent virus infection.

However, such NP-promoted LCMV transmission via keratin network-supported connections could be helpful not only for the spread of persistent LCMV infection. It is also possible that a similar transmission route can be utilized by mature LCMV virions in epithelial tissues composed of cells containing the keratin network, such as airway or gastric epithelial cells, which serve as natural entry portals for LCMV infection in vivo (5, 36). This can represent a mechanism complementing conventional virion release and maximizing the spread of virions to neighboring noninfected epithelial cells.

In conclusion, based on the data obtained in this study, we propose that LCMV facilitates its cell-cell spread in persistently infected HeLa cells via a mechanism that involves NP binding and manipulation of K1 and results in increased formation of intercellular contacts. Although the proposed mechanism shares fundamental aspects with the actin-related mechanisms utilized by other viruses during noncytolytic infections, it provides new insight into the biological consequences of virus-host cell interaction.

ACKNOWLEDGMENTS

This work was supported by grants from the Scientific Grant Agency of the Ministry of Education of the Slovak Republic and the Slovak Academy of Sciences (VEGA-2/5081/05) and from the State Program of Research and Development (SP 51/028 08 00/028 08 03).

We thank Anna Ohrad'anová for help with cloning into pGEX plasmids, Alzbeta Hulíková for help with microscopy and picture processing, and Juraj Petrik for critical reading of the manuscript.

REFERENCES

1. **Amman, B. R., B. I. Pavlin, C. G. Albariño, J. A. Comer, B. R. Erickson, J. B. Oliver, T. K. Sealy, M. J. Vincent, S. T. Nichol, C. D. Paddock, A. J. Tumpey, K. D. Wagoner, R. D. Glauer, K. A. Smith, K. A. Winpisinger, M. S. Parsely, P. Wyrick, C. H. Hannafin, U. Bandy, S. Zaki, P. E. Rollin, and T. G. Ksiazek.** 2007. Pet rodents and fatal lymphocytic choriomeningitis in transplant patients. Emerg. Infect. Dis. **13:**719–725.
2. **Buchmeier, M. J.** 2002. Arenaviruses: protein structure and function. Curr. Top. Microbiol. Immunol. **262:**159–173.
3. **Chidgey, M., and C. Dawson.** 2007. Desmosomes: a role in cancer? Br. J. Cancer **96:**1783–1787.
4. **Diefenbach, R. J., M. Miranda-Saksena, E. Diefenbach, D. J. Holland, R. A. Boadle, P. J. Armati, and A. L. Cunningham.** 2002. Herpes simplex virus tegument protein US11 interacts with conventional kinesin heavy chain. J. Virol. **76:**3282–3291.
5. **Dylla, D. E., D. E. Michele, K. P. Campbell, and P. B. McCray, Jr.** 2008. Basolateral entry and release of New and Old World arenaviruses from human airway epithelia. J. Virol. **82:**6034–6038.
6. **Favoreel, H. W., G. van Minnebruggen, D. Adriaensen, and H. J. Nauwynck.** 2005. Cytoskeletal rearrangements and cell extensions induced by the US3 kinase of an alphaherpesvirus are associated with enhanced spread. Proc. Natl. Acad. Sci. USA **102:**8990–8995.
7. **Fischer, S. A., M. B. Graham, M. J. Kuehnert, C. N. Kotton, A. Srinivasan, F. M. Marty, J. A. Comer, J. Guarner, C. D. Paddock, D. L. DeMeo, W. J. Shieh, B. R. Erickson, U. Bandy, A. DeMaria, Jr., J. P. Davis, F. L. Delmonico, B. Pavlin, A. Likos, M. J. Vincent, T. K. Sealy, C. S. Goldsmith, D. B. Jernigan, P. E. Rollin, M. M. Packard, M. Patel, C. Rowland, R. F. Helfand, S. T. Nichol, J. A. Fishman, T. Ksiazek, S. R. Zaki, and the LCMV in Transplant Recipients Investigation Team.** 2006. Transmission of lymphocytic choriomeningitis virus by organ transplantation. N. Engl. J. Med. **354:**2235–2249.
8. **Gerdes, H.-H., N. V. Bukoreshtliev, and J. F. Barroso.** 2007. Tunneling nanotubes: a new route for the exchange of components between animal cells. FEBS Lett. **581:**2194–2201.
9. **Gibadulinová, A., V. Zelník, L. Reiserová, E. Závodská, M. Zat'ovičová, F. Ciampor, S. Pastoreková, and J. Pastorek.** 1998. Sequence and characterisation of the Z gene encoding ring finger protein of the lymphocytic choriomeningitis virus MX strain. Acta Virol. **42:**369–374.
10. **Gill, M. B., R. Edgar, J. S. May, and P. H. Stevenson.** 2008. A gammaherpesvirus glycoprotein complex manipulates actin to promote viral spread. PLoS One **3:**1–12.
11. **Green, K. J., B. Geiger, J. C. R. Jones, J. C. Talian, and R. D. Goldman.** 1987. The relationship between intermediate filaments and microfilaments prior to and during the formation of desmosomes and adherens-type junctions in mouse epidermal keratinocytes. J. Cell Biol. **104:**1389–1402.
12. **Green, K. J., and C. L. Simpson.** 2007. Desmosomes: new perspectives on a classic. J. Investig. Dermatol. **127:**2499–2515.
13. **Hasan, A. A. K., T. Zisman, and A. H. Schmaier.** 1998. Identification of cytokeratin 1 as a binding protein and presentation receptor for kininogens on endothelial cells. Proc. Natl. Acad. Sci. USA **95:**3615–3620.
14. **Hernychova, L., R. Toman, F. Ciampor, M. Hubalek, J. Vackova, A. Macela, and L. Skultety.** 2008. Detection and identification of *Coxiella burnetii* based on the mass spectrometric analyses of the extracted proteins. Anal. Chem. **80:**7097–7104.
15. **Jahrling, P. B., and C. J. Peters.** 1992. Lymphocytic choriomeningitis virus. A neglected pathogen of man. Arch. Pathol. Lab. Med. **116:**486–488.
16. **Jamieson, D. J., A. P. Kourtis, M. Bell, and S. A. Rasmussen.** 2006. Lymphocytic choriomeningitis virus: an emerging obstetric pathogen? Am. J. Obstet. Gynecol. **194:**1532–1536.
17. **Johnson, D. C., and M. T. Huber.** 2002. Directed egress of animal viruses promotes cell-to-cell spread. J. Virol. **76:**1–8.
18. **Magin, T. M., P. Vijayaraj, and R. E. Leube.** 2007. Structural and regulatory functions of keratins. Exp. Cell Res. **313:**2021–2032.
19. **Meyer, B. J., J. C. de la Torre, and P. J. Southern.** 2002. Arenaviruses: genomic RNAs, transcription, and replication. Curr. Top. Microbiol. Immunol. **262:**139–157.
20. **Oldstone, M. B.** 2002. Biology and pathogenesis of lymphocytic choriomeningitis virus infection. Curr. Top. Microbiol. Immunol. **263:**83–117.
21. **Pastorekova, S., Z. Zavadova, M. Kostal, O. Babusikova, and J. Zavada.** 1992. A novel quasi-viral, MaTu, is a two-component system. Virology **187:**620–626.
22. **Peters, C. J., M. Buchmeier, P. E. Rollin, and T. G. Ksiazek.** 1996. Arenaviruses, p. 1521–1552. *In*: B. N. Fields, D. M. Knipe, and P. M. Howley (ed.) Fields virology, 3rd ed. Lippincott-Raven Publishers, New York, NY.
23. **Pinschewer, D. D., M. Perez, and J. C. de la Torre.** 2003. Role of the virus nucleoprotein in the regulation of lymphocytic choriomeningitis virus transcription and RNA replication. J. Virol. **77:**3882–3887.
24. **Radtke, K., K. Döhner, and B. Sodeik.** 2006. Viral interactions with the cytoskeleton: a hitchhiker's guide to the cell. Cell. Microbiol. **8:**387–400.
25. **Reiserova, L., M. Kaluzova, S. Kaluz, A. C. Willis, J. Zavada, E. Zavodska, Z. Zavadova, F. Ciampor, J. Pastorek, and S. Pastorekova.** 1999. Identification of MaTu-MX agent as a new strain of lymphocytic choriomeningitis virus (LCMV) and serological indication of horizontal spread of LCMV in human population. Virology **257:**73–83.
26. **Salvato, M. S., and E. M. Shimomaye.** 1989. The completed sequence of lymphocytic choriomeningitis virus reveals a unique RNA structure and a gene for a zinc finger protein. Virology **173:**1–10.
27. **Shabana, A. H., M. Oboeuf, and N. Forest.** 1994. Cytoplasmic desmosomes and intermediate filament disturbance following acrylamide treatment in cultured rat keratinocytes. Tissue Cell **26:**43–55.
28. **Sherer, N. M., and W. Mothes.** 2008. Cytonemes and tunneling nanotubules in cell-cell communication and viral pathogenesis. Trends Cell Biol. **18:**414–420.
29. **Sherer, N. M., M. J. Lehmann, L. F. Jimenez-Soto, C. Horensavitz, M. Pypaert, and W. Mothes.** 2007. Retroviruses can establish filopodial bridges for efficient cell-to-cell transmission. Nat. Cell Biol. **9:**310–315.
30. **Southern, P. J., M. K. Singh, Y. Riviere, D. R. Jacoby, M. J. Buchmeier, and M. B. Oldstone.** 1987. Molecular characterisation of the genomic S RNA segment from lymphocytic choriomeningitis virus. Virology **157:**145–155.
31. **Sowinski, S., C. Jolly, O. Berninghausen, M. A. Purbhoo, A. Chauveau, K. Köhler, S. Oddos, P. Eissmann, P. M. Brodsky, C. Hopkins, B. Önfelt, Q. Sattentau, and D. M. Davies.** 2008. Membrane nanotubes physically connect T cells over long distances presenting a novel route for HIV-1 transmission. Nat. Cell Biol. **10:**211–219.
32. **Tomaskova, J., M. Labudova, J. Kopacek, S. Pastorekova, and J. Pastorek.** 2008. Molecular characterization of the genes coding for glycoprotein and L protein of lymphocytic choriomeningitis virus strain MX. Virus Genes **37:**31–38.
33. **van der Zeijst, B. A. M., B. E. Noyes, M. E. Mirault, B. Parker, A. D. M. E. Osterhaus, E. A. Swyryd, N. Bleumink, M. C. Horzinek, and G. R. Stark.** 1983. Persistent infection of some standard cell lines by lymphocytic choriomeningitis virus: transmission of infection by an intracellular agent. J. Virol. **48:**249–261.
34. **Windoffer, R., A. Kölsch, S. Wöll, and R. E. Leube.** 2006. Focal adhesions are hotspots for keratin filament precursor formation. J. Cell Biol. **173:**341–348.
35. **Wolffe, E. J., A. S. Weisberg, and B. Moss.** 1998. Role of vaccinia virus A36R outer envelope protein in formation of virus-tipped actin-containing microvilli and cell-to-cell virus spread. Virology **244:**20–26.
36. **Yin, C., M. Djavani, A. R. Schenkel, D. S. Schmidt, C. D. Pauza, and M. S. Salvato.** 1998. Dissemination of lymphocytic choriomeningitis virus from the gastric mucosa requires G protein-coupled signaling. J. Virol. **72:**8613–8619.